6-2008

A Comparative Analysis of Pixel-Based and Object-Oriented Image Analysis Methods Using Landsat Imagery

Jason Joseph Delisio

A COMPARATIVE ANALYSIS OF PIXEL-BASED AND OBJECT-ORIENTED IMAGE ANNALYSIS METHODS USING LANDSAT IMAGERY

by

Jason Joseph Delisio

A Thesis
Submitted to the
Faculty of The Graduate College
in partial fulfillment of the
requirements for the
Degree of Master of Arts
Department of Geography

Western Michigan University
Kalamazoo, Michigan
June 2008

ACKNOWLEDGEMENTS

First and foremost I would like to thank my advisor, Dr. Charles Emerson for guiding and supporting me through the process of researching and writing this thesis. It was under his instruction that I learned and became familiar with many of the methods used in this study and I appreciate his time and effort. I would also like to thank the rest of my committee: Dr. Chansheng He for his guidance in selecting a thesis topic and the process of writing a thesis and Dr. Gregory Veeck for his support and willingness to share his knowledge about China. I want to thank the rest of the faculty and students of the Department of Geography at Western Michigan University for their friendship and encouragement during the process whether through a kind word or constructive criticism. Additionally, I would like to thank the faculty of the Department of Geography at Youngstown State University who, by and large, prepared me for graduate school and cared enough to continue to check on me and encourage me even after I graduated. I also thank Dr. Matthew Hansen of South Dakota State University, whose research internship helped me to develop the technical skills to carry of much of this thesis as well as the research skills necessary. I thank Dr. Li Zhou and his colleagues at the Rural Development Institute (RDI) of the Chinese Academy of Social Sciences (CASS) for providing me with some of the data used in this study. I want to also acknowledge the National Science Foundation (NSF) Geography and Regional Science grant (#0616763) which provided funding for the Landsat imagery.

Finally, I would like to thank my family for their love and support as I pursued my degree, my friends who constantly encouraged and pushed me, and my fiancé, Michelle for her love and hard work that always inspired me to do my best. Thank you all again, without your help none of this would have been complete.

Jason J. Delisio

A COMPARATIVE ANALYSIS OF PIXEL-BASED AND OBJECT-ORIENTED IMAGE ANALYSIS METHODS USING LANDSAT IMAGERY

Jason Joseph Delisio, M.A.

Western Michigan University, 2008

Pixel-based and object-oriented image analysis methods are two popular techniques for classifying satellite imagery. Pixel-based analysis is typically used for coarser resolution imagery while object-oriented analysis is ideal for high resolution imagery. However, the ability of object-oriented image analysis to segment images based on factors such as shape, color, texture, and spatial attributes suggest that it can perform as well or better than pixel-based analysis in classifying medium resolution imagery. A comparative analysis of the two methods was performed using Landsat 5 Thematic Mapper imagery from September 2006 to classify grassland quality and land cover in Da'erhanmaoming'an (DaMao) Banner, Inner Mongolia, China. After calculating a Normalized Difference Vegetation Index (NDVI) for each of the three images, a supervised classification was performed separately using the two methods. Land cover classes included three types of grassland (good, average, poor), built up/urban areas, agriculture, and barren. It was found that the object-oriented methodology produced higher overall accuracy and KHAT percentages in all three images. The highest achieved accuracy for the object-oriented technique was 84.93% with a KHAT of 0.8006 while the highest accuracy for the pixel-based technique for the pixel based technique was 82.83% with a KHAT of 0.697

TABLE OF CONTENTS

Table of Contents----continued

CHAPTER

LIST OF TABLES

LIST OF FIGURES

CHAPTER 1
INTRODUCTION

1.1 Background

When trying to develop an understanding of the impacts of humans on the environment it is important to be able to observe and study the changes in land use/land cover over multiple periods of time and over a large spatial extent. Phenomena such as deforestation and grassland degradation are two examples of these changes that are being studied around the world. In order to better assess the extent of land use/land cover changes, remote sensing image analysis methods have been developed to observe, classify and map these changes using satellite imagery. Two popular methods used today are pixel-based image analysis and object-oriented image analysis. This thesis will conduct a comparative analysis of these two methods to classify land use/land cover and assess grassland quality in Da'erhanmaoming'an (DaMao) Banner, Inner Mongolia Autonomous Region (IMAR), Peoples Republic of China.

Traditionally, pixel-based methods have been used in the majority of remotely sensed image analyses. Pixel-based analysis is a statistical clustering method in which pixels are individually sampled within an image to create a set of samples that are used to classify land use/land cover in an image. For example, if a pixel is classified as representing a particular type of grassland, water, or urban land cover, the value of that pixel, and similar sample pixels, will then be used to classify the rest of the image (Jensen 2005). Studies, such as Townshend et al. (2000) point out some of the problems that exist with using "per pixel" methods, such as problems associated with interference from one signal value influencing neighbor pixels. When this type of "mixing" occurs along a boundary, it would seem inappropriate to assign any of the boundary pixels to an

exclusive class (Shanmugam et. al. 2003). Because this method deals with individual pixels, it is better suited for medium resolution imagery, such as images from Landsat series of satellites (30m ground resolution), as well as course resolution imagery such as Advanced Very High Resolution Radiometer (AVHRR) (1.1 km) and the Moderate Resolution Imaging Spectroradiometer (MODIS) (500m).

In contrast, the basis of object-oriented image analysis is a segmentation process which allocates pixels to homogeneous, multi-pixel image objects. Segmenting an image allows for analysis using characteristics such as texture, spatial qualities, or contextual relationships instead of only spectral signatures, which theoretically can create a better classification. In Baatz et. al. (2004) much of the discussion is based on how object-oriented analysis (through the eCognition™ software) is best suited for very high resolution (VHR) imagery, such as the images provided by IKONOS or SPOT, which both have resolutions of less than 5m. Individual objects in a higher resolution image consist of multiple homogeneous pixels, which object-oriented analysis attempts to separate. However, in an application such as this, object-oriented analysis could be useful due to the nature of land use in the study region. The areas of grasslands, agriculture, urban, and water are often large and have distinctive shapes and texture that object-oriented analysis can potentially "recognize" and segment.

When comparing the two analysis methods there are distinct advantages and. Object-oriented analysis operates on the assumption that "information necessary to interpret an image is not represented in single pixels, but rather in meaningful image objects and their mutual relations" (Yijun and Hussin 2003). This ability to consider the collective attributes of objects instead of the single attributes of individual pixels is the

biggest advantage that object-oriented analysis has over pixel-based methods. Yijun and Hussin (2003) make the claim that object-oriented analysis leads to higher classification accuracy and better semantic differentiation.

There are a few disadvantages to object-oriented analysis. One disadvantage is that object-oriented analysis is primarily designed for use on very high resolution imagery. However, the works of Cui and Hussin (2003) suggest that object-oriented analysis can be applied to medium resolution imagery, such as that provided by Landsat 5. Another disadvantage is that figuring out a set of segmentation parameters that works best is a time consuming, heuristic process because there are no deductive definitions that exist.

The advantage of a pixel-based approach is that information is not lost in the classification process. Object-oriented analysis generalizes some of the information in images in order to group pixels into image objects. This generalization causes a loss of information (Erasmi et. al. 2004). On the other hand Erasmi et. al. (2004) point out that "pixel-based classifications always face the problem of mixed pixels as well as salt and pepper features and thus, in most cases, require pre- and post-classification smoothing".

So when classifying the grassland areas of DaMao Banner, IMAR, China what is the best method to use? Both of these methods have advantages and disadvantages when it comes to mapping and assessing change of phenomena in a satellite image. This study will focus on a comparative analysis of the performance of each of these methods to see if one method is superior to the other for this type of application. Knowledge of this is important for resource management officials, for future research into grassland quality, as well as for modeling agricultural land use changes in IMAR.

The primary research objective then, will be to conduct a comparative analysis on how pixel-based and object-oriented methods perform when classifying grassland quality and land cover in the Inner IMAR of China using imagery from the United States' Landsat 5 satellite. Within the context of conducting a comparative analysis, results of an accuracy assessment, as well as evaluations of the visual quality of classifications and processing time will be considered in finding which method best suits this application. The images will be classified into seven land cover classes which will include urban/built up, water, agriculture, barren, and good, average, and poor grasslands.

1.2 Structure of Thesis

This thesis will be structured as follows. Chapter 2 is a literature review of studies that provide background and guide this research. The topics covered in the literature are grasslands, similar comparative studies, and vegetation indices. Chapter 3 focuses on methodology and contains a more in-depth look at the study area and the steps taken to prepare and analyze the satellite images. Chapter 4 discusses the results and contains explanations of the importance of the findings in the error matrices. Chapter 5 brings the thesis to a close with a summary of the work done and the findings as well as a discussion of future research.

CHAPTER 2
LITERATURE REVIEW

Grasslands are vital ecosystems in all parts of the world and as such, the changes in them are being monitored and evaluated through numerous studies in many different countries. This literature review will be separated into three sections. The first section will discuss important aspects of grasslands such as their economic and ecological importance as well as the human practices that are destroying them in parts of the world. More specifically, the focus of review will be the issue of animal husbandry practices as they relate to overgrazing of grasslands. The second section will review pixel-based and object-oriented techniques in studies that relate to grassland and resource management. The third section will take a look at different vegetation indices and how they are used in various remote sensing studies.

2.1 Grasslands

Grasslands are diverse ecosystems that exist in most regions of the world. By some measurements land cover defined as grassland covers approximately 40% of the earth's surface, excluding Greenland and Antarctica (White et. al. 2000). Grasslands are semi-arid regions that contain herbaceous and shrub vegetation and are maintained by fire, grazing, drought, or freezing temperatures (White et. al. 2000, Laliberte et. al. 2004, and Di Bella et. al. 2005). In addition to the diversity of wildlife that grasslands support, they are also important to the economies of many countries. China, Argentina, the United States, Australia and countries throughout the European Union use grasslands for economic activities such as agriculture and livestock grazing.

With the growing demand for products and services in rapidly developing countries like China, and India, further demand is being placed on grasslands (Veeck et. al. 2007). Desertification, which happens when land cover changes to desert is a widespread problem in grassland regions The degradation of these grasslands, caused by overgrazing, farming and climatic changes due to global warming, are major issues that are being researched around the world (Di Bella et. al 2005 and Paruelo and Lauenroth 1995). Overgrazing of grasslands for economic purposes is an unsustainable practice that, despite economic positives in the short term, has distinct consequences in the long term, such as decline of productivity and increase in poverty (Veeck et. al. 2007 and Milton, et. al. 1994). Thankfully, because of modern innovation grasslands can be monitored like never before. The development of better satellites and the advancement of image analysis methodologies allow for grasslands to be studied on regional and global scales far more effectively than in the past.

The "ongoing land degradation process" in the arid steppe regions of Northern China was researched using satellite imagery in a study conducted by Brogaard et. al. (2005). In this study the researchers use a Light Use Efficiency (LUE) model to assess biological production with the grasslands. A LUE is a model that uses the amount of photosynthetically active radiation absorbed by vegetation as a measurement of biological production. A measured decline in biological production is an indicator of desertification in a grassland region.

Another type of grassland degradation issue is shrub encroachment. Increased shrub cover leads to declines in "species diversity, water availability, grazing capacity, and soil organic matter" (Laliberte et. al. 2004). Using aerial photos and QuickBird

satellite imagery, Laliberte et. al. (2004) utilized an object-oriented image analysis to map the path of shrub encroachment in New Mexico from 1937 to 2003. The object-oriented methodology used in this study will be discussed in greater detail in section 2.2 of this chapter, however the use of this methodology for grassland applications is important to note.

A study by Zha et. al. (2003) combined ***in situ*** ground measurements collected using a spectrometer with Normalized Difference Vegetation Index (NDVI) measurements from Landsat TM imagery to quantify grassland cover. The ability to measure grassland cover from year to year is an important process in monitoring the health of grasslands. The methods used in Zha et. al. (2003) quantified grasslands in the study area with an overall accuracy of 89%. The classification method used in this study was a pixel-based method. Object-oriented and pixel based methods have both been used to monitor grasslands using satellite imagery. Section 2.3 of this chapter will focus on how the literature defines the methods and how they compare in studies.

2.2 Vegetation Indices

Vegetation indices can be defined as spectral band combinations that "account for varying atmospheric conditions and eliminate soil background contribution in estimating vegetation responses" (Navulur 2007). The three most popular vegetation indices are the Ratio Vegetation Index (RVI), the Normalized Difference Vegetation Index (NDVI), and the Soil Adjusted Vegetation Index (SAVI) (Navulur 2007, Schowengerdt 1997).

The most basic of these indices is the RVI. This index divides the Near-Infrared (NIR) by the red band in order to indicate vegetation in an image (Navulur 2007, Schowengerdt 1997). The equation for this index is:

$$RVI = DN_{NIR} / DN_{Red} \quad \text{[Equation 1]}$$

where DN represents the digital number, or the value, of a pixel in the NIR and red bands respectively. This equation creates a wide range of possible values varying from approximately 1 for bare soil to greater than 20 for dense vegetation (Navulur 2007).

NDVI is perhaps the most popular of the vegetation indices because it "compensates for different amounts of light and produces a number between 1 and -1" with ranges of values vary between 0.1 for bare soils to 0.9 for dense vegetation, such as forests and woodlands (Navulur 2007). One of the primary uses for the NDVI is to monitor vegetation on "continental and global scales". The equation for the NDVI is:

$$NDVI=(P_{NIR}-P_{RED})/(P_{NIR}+P_{RED}) \quad \text{[Equation 2]}$$

However, Schowengerdt (1997) states that the NDVI "appears to be a poor indicator of vegetation biomass if the ground cover is low, as in arid and semi-arid regions". Additionally Campbell (2002) points out that ratios, such as the NDVI, must be used carefully since they can be easily influenced by "factors external to the plant leaf" such as viewing angle, soil, and path radiance from suspended particles in the atmosphere atmospheric.

While NDVI is more useful on forested ground cover, SAVI is noted as a "superior" vegetation index for low cover environments, such as grasslands

(Schowengerdt 1997). SAVI is similar to the NDVI but adds some terms to adjust for different brightness values of background soil (Navulur 2007). The equation for SAVI is:

$$SAVI = ((P_{NIR} - P_{Red})/(P_{NIR} + P_{Red} + L))(1 + L) \quad \text{[Equation 3]}$$

If L is zero then SAVI is the same as the NDVI but in most cases L is given a value of 0.5 (Navulur 2007, Schowengerdt 1997).

In many of the studies that require a vegetation index the one that is most widely used is NDVI. Despite the limitations of the NDVI on low biomass land cover types found in arid and semi-arid regions, such as grasslands, there are still many studies that make use of this index for many different purposes. In Paruelo and Lauenroth (1995), NDVI values are derived using spectral data from the National Oceanic and Atmospheric Administration/Advanced Very High Resolution Radiometer (NOAA/AVHRR) satellites in order to describe the functional characteristics of North American shrublands and grasslands on a regional scale. Zha et. al. (2003) concludes that NDVI measurements derived from Landsat TM imagery can be used to reliably quantify grass cover.

2.3 Comparative Studies of Techniques

In recent years the amount of research being published comparing pixel-based and object-oriented techniques using medium resolution imagery has increased. Researchers appear to recognize the theoretical advantages of object-oriented classifications and thus, want to test it against traditional methods (Santos et. al 2006). Traditionally, pixel-based methods are used to classify medium and course resolution imagery. Two of the primary methods for doing this are unsupervised and supervised classification. The difference between the two is that in unsupervised classification a computer algorithm is used to

define heterogeneous clusters of similar spectral signatures inductively. The user then assigns these clusters to land cover classes. On the other hand, supervised classification is a method in which the user selects "training" samples of homogeneous pixels to represent predefined classes. The spectral signatures from the sample are then used to classify the remainder of unclassified pixels in the image (Schowengerdt 1997). The sampled signatures are applied to the rest of the unclassified pixels through a number of statistical processes. For example, in Santos et. al. (2006) a Gaussian Maximum Likelihood classifier is used. This type of classifier is referred to as a "hard" classifier. A maximum likelihood classification is based upon the estimation of class membership for an unknown pixel using multivariate normal distribution models for the classes (Schowengerdt 1997). This method considers the variability of classes by evaluating the variance and covariance of the training signatures when classifying an unknown pixel (Shanmugam et. al. 2003). This is one of the most widely used classifiers because of its simplicity and robustness (Platt and Goetz 2004).

While pixel-based analysis relies solely on spectral and statistical information in each of the pixels, object-oriented analysis attempts to classify an image based on homogeneous image objects (Platt and Rapoza 2008). Definiens Professional™ (formerly known as eCognition™) is a commercially available software package used to conduct object-oriented image analysis. The first step of object-oriented analysis is a process called multiresolution segmentation. During this process, an image is segmented into groups of homogeneous image objects based on a series of user defined spectral and spatial qualities (such as shape, size, and edges). In Definiens Professional™ there are five parameters that need to be set to begin the segmentation process. The first is the (1)

scale factor. This parameter is a unitless number that determines the size of the image objects. As the scale factor increases the objects generally get larger. The next two factors are paired together on a sliding scale from zero to one. (2) Color and (3) Shape are parameters that determine the spectral heterogeneity of the objects. (4) Compactness and (5) Smoothness are also paired together on a sliding scale from zero to one. These parameters control the shape of the segmented objects (Baatz et. al. 2004 and Platt and Rapoza 2008). The process of adjusting these parameters is a heuristic process in which no "optimal" standard exists (Benz et. al. 2004).

The classification of image objects is similar to pixel-based supervised classification. Objects can be sampled and applied to predefined classes. A major difference however is that classes and objects can be hierarchical, meaning a grassland class can be broken down into multiple sub-classes of grassland. Because of the ability of object-oriented analysis to segment an image on several levels using multiple scales, smaller objects at lower levels can nest into larger objects at high levels of the hierarchy. Objects can also be assigned to classes using a rule-based classification process which allows the user to create a decision tree of rules to define class membership, but this is described as a more time consuming process (Kressler et. al. 2005). In Definiens, classification is done using a nearest-neighbor classifier. This classifier assigns objects to the class that is closest to it in feature space (Platt and Rapoza 2008).

In Santos et. al. (2006) the two techniques are applied to map land cover of Portugal using Envisat Medium Resolution Imagery Spectrometer (MERIS) from the European Space Agency (ESA). For the pixel-based classification procedure a Maximum Likelihood (ML) supervised classifier was used. The supervised classification was

applied to three separate images independently using ENVI 4.1 software and in order to classify all pixels a probability threshold was not applied to any of the images.

For the object-oriented portion of the study a two step approach was used: segmentation of the image and classification of the image objects. In this study the researchers weighted color and shape and compactness and smoothess evenly by setting each parameter to 0.5 and used a scale factor of 10. The researchers used a satellite derived NDVI layer to classify vegetation classes and used a rule-based classification process to classify vegetation as anything with a value greater than zero. A combination of sample objects and the rule-based classification concept was done in order to build up the knowledge base for the classification of image objects. Overall the study found that traditional pixel-based procedures produced better results when applied to medium resolution imagery, such as MERIS. The map that used the pixel-based process with a maximum likelihood classifier rated a KHAT (which is an indication of how much better than chance the results are) of 85% against a KHAT of 63% for the object-oriented classifier. The researchers concluded that the quality results of the object-oriented classifier were also inferior to those produced by the maximum likelihood classifier.

Platt and Rapoza (2008) also conducted a study to examine the extent to which the object-oriented analysis increases land use/land cover classification accuracy over traditional pixel based methods. The researchers used eight total classification models: four pixel-based models and four object-oriented models. In each of the models they changed several factors including the classifier (nearest-neighbor or maximum likelihood), the use of expert knowledge, and the type of feature space (spectral or optimized). The authors based their comparison on the error matrices, weighted

agreement, and weighted disagreement location, and quantity. The weighted agreement and disagreement is defined in the study as the percent correct weighted by the actual occurrence in the landscape as estimated by the number of points in the random sample. The authors used eCognition™ for their object-oriented analysis and concluded that the object-oriented methodology yielded a considerable improvement over traditional pixel-based methods for the images used. They also found that the ability to analyze on the object level, the use of the nearest-neighbor classifier, and expert knowledge, are the factors that yield the highest classification accuracy.

A review of the literature shows mixed results and existing work still does not clearly show whether object-oriented analysis and all its theoretical advantages can actually produce more accurate results when used with medium resolution imagery. It is this on-going debate that has stimulated the current research.

CHAPTER 3
STUDY AREA AND METHODOLOGY

3.1 Study Area

The study area for this research is Da'erhanmaoming'an (DaMao) Banner in north-central China (Figure 3.1). The banner (an administrative division similar to a county in the United States) borders the country of Mongolia to the north and is one of the 101 political subdivisions of Inner Mongolian Autonomous Region (IMAR). DaMao is situated in one of Eurasia's most ecologically sensitive arid and semi-arid regions and, along with neighboring banners, contains 17% of the IMAR's grasslands (Veeck et. al. 2007). The banner is sparsely populated with a 2006 population of 101,301 and an area of 17,410 km^2 (Inner Mongolia Statistical Year Book 2007). As of 1997, DaMao was one of 31 "state-identified poverty banners and counties" in the IMAR region with 31.4% of the population classified as "poor" (Inner Mongolia Project Management Office 1998). The primary economic activities of DaMao and surrounding banners are agriculture and animal husbandry, but the development of these activities is hindered due to the remote location of the banner as well "inconvenient" communication caused by inadequate transportation options (Inner Mongolia Project Management Office 1998). Table 3.1 shows a comparison of economic and livestock statistics for DaMao Banner and several surrounding banners with totals and averages for the entirety of the IMAR as well.

Figure 3.1 Map of the Study area

Table 3.1 Comparison of livestock density and per capita income

Banner	Livestock (Head)	Area (sq km)	Density (head/sq km	Per capita Income
Wulatezhong	1,117,200	22,606	49.42	2,447
DaMao	**753,200**	**17,410**	**43.26**	**1,576**
Siziwang	865,400	24,016	36.03	1,615
Suniteyou	613,400	26,700	22.97	845
Sunitezou	793,000	33,469	23.69	1,728
Abaga	1,198,200	27,495	43.58	2,430
IMAR totals	44,951,000	1,183,000	38.00	2,086

Source: Inner Mongolian Statistical Yearbook, 2004

Table 3.1 shows that DaMao has the third highest livestock density in the region but has the second lowest per capita income, well below the average of the rest of IMAR. Because of the strain placed of the grasslands of this region due to the amount of livestock, several environmental problems have come to the forefront in recent years, including grassland degradation. However, these problems have become the focus of increased research activity (Veeck et. al. 2007). Three Landsat 5 scenes from the United State Geological Survey (USGS) are needed to view the entire study area. Landsat 5 scenes are labeled based on their path and row numbers. Paths and rows are similar to columns and rows in a grid, respectively. For this study the images used were as follows: path 127 row 31, path 128 row 30, and path 128 row 31. Figure 3.2 shows the outlines of the Landsat 5 scenes over DaMao.

3.2 Methods

The first step in classifying imagery, regardless of what method is being used, is to prepare the image for processing.

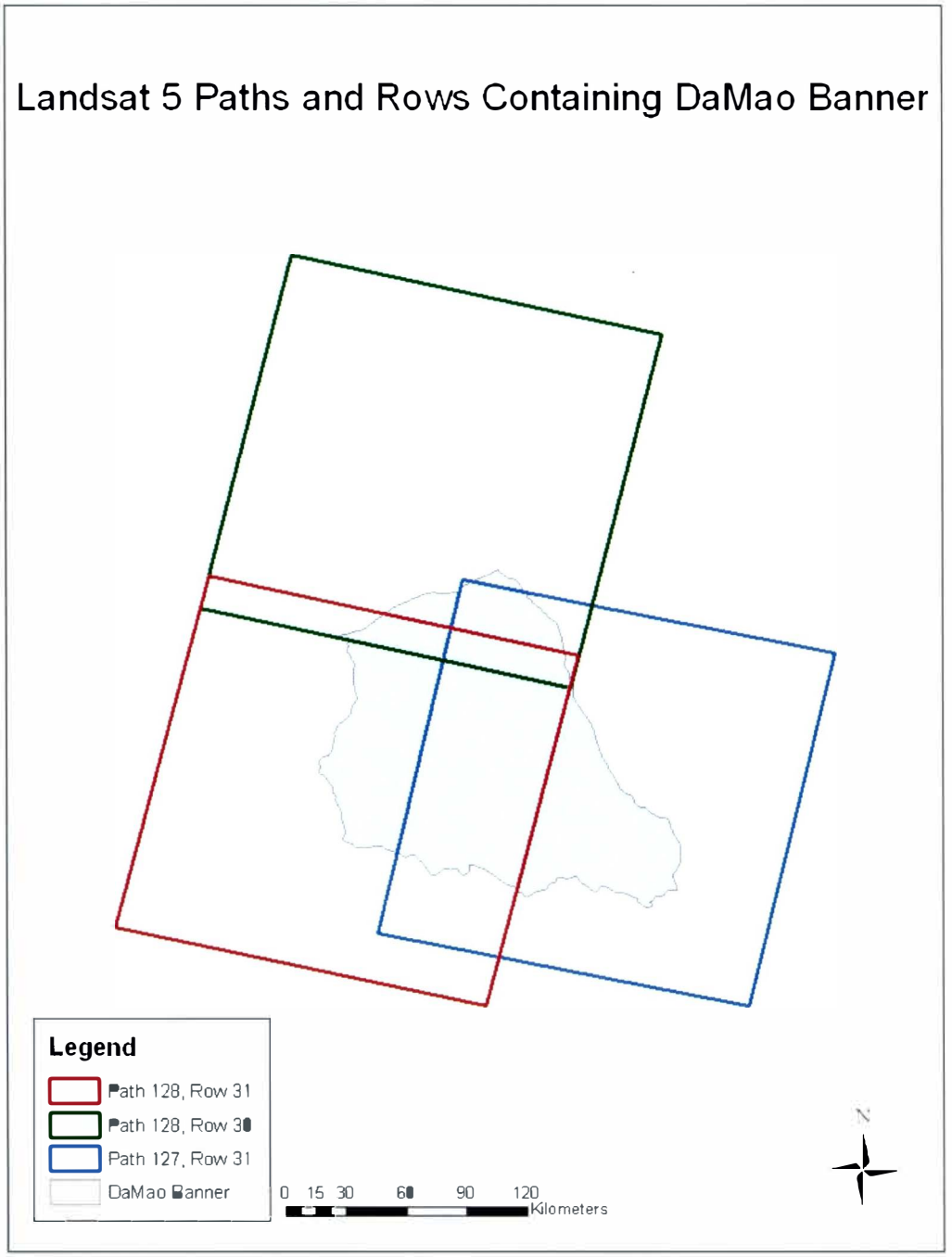

Figure 3.2 Outlines of Landsat 5 scenes overlaid on DaMao Banner

For the purposes of this research, the first step in preparing the imagery was to convert the image digital numbers, which are unitless values, to spectral radiance values, which are units of absolute radiance. The equation for the conversion from digital numbers to spectral radiances is:

$$L_A = G_{rescale} \times Q_{cal} + B_{rescale} \quad \text{[Equation 4]}$$

where "L_A" is the spectral radiance measured in $W/m^2/sr/\mu m$, "Q_{cal}" is the quantized calibrated pixel value of the digital numbers, G is the gain and B is the offset, which are sensor specific conversion values that are contained in the image header (Chander and Markham 2003). Table 3.2a contains all the input parameters that are used to convert an image from raw digital numbers to radiances. The data in this table are for Landsat 5 images taken after May 5, 2003.

Table 3.2a Landsat 5 TM postcalibration dynamic ranges

Spectral Radiences, $LMIN_A$ and $LMAX_A$ in $W/m^2.sr.\mu m$

Band	LMIN	LMAX	$G_{rescale}$	$B_{rescale}$
1	-1.52	193	0.762824	-1.52
2	-2.84	365	1.44251	-2.84
3	-1.17	264	1.03988	-1.17
4	-1.51	221	0.872588	-1.51
5	-0.37	30.2	0.119882	-0.37
6	1.2378	15.303	0.055158	1.2378
7	-0.15	16.5	0.065294	-0.15

Next, the radiance values can be converted to planetary reflectance values. This is a normalization process that converts the radiances to percentages using sun angle and atmospheric reflections. This normalization creates a reduction in between-scene variability which provides calibrated, consistent measurements across each of the images that were used (Chander and Markham 2003).

Table 3.2b Radiance parameters for study images

Image	Date	Landsat	DOY	SolarDist	SD^2	Solar Elev	Zenithradians	B4 Gain	B4 Offset	Red Gain	Red Offset	B4 ESUN	Red ESUN
p128r30	9/1/2006	5	244	1.0088	1.018	57.81	0.561821486	0.8726	-1.51	1.03988	-1.17	103.6	155.4
p128r31	9/1/2006	5	244	1.0088	1.018	51.88	0.665319511	0.8726	-1.51	1.03988	-1.17	103.6	155.4
p127r31	9/10/2006	5	254	1.0066	1.013	49.17	0.712617934	0.8726	-1.51	1.03988	-1.17	103.6	155.4

Spectral reflectance values are calculated by taking into consideration the earth-sun distance and the solar zenith angle on the day the image was taken. Table 3.2b shows the parameters that are used to convert radiance

values to planetary reflectances, including day of year (DOY), solar distance, solar elevation, and zenith radians. The equation for the conversion of spectral radiance to at-satellite reflectance is:

$$\rho_p = (\pi * L_\lambda * d^2) / (ESUN_\lambda * \cos\theta_s) \quad \text{[Equation 5]}$$

where:

ρ_p =at-satellite planetary reflectance (unitless)

L_λ =Spectral radiance at sensor aperture in $mW*cm^{-2}*ster^{-1}*\mu m^{-1}$ for band λ

d =Earth-sun distance in astronomical units

$ESUN_\lambda$ =Mean solar exoatmospheric for band λ irradiances from table 3.2b

θ_s =Solar zenith angle in degrees

Both of these conversion processes are easily done using tools in commercial software, such as ENVI™ 4.2, that use the header file for each image to determine the date the image was taken and then enters the correct parameters for that day.

Typically, the next step is to mosaic the images that make up a study area and clip them using an outline of the study area. In this project each of the three Landsat 5 scenes that were used contained certain characteristics that led to the idea that, for comparisons sake, it was better to consider each scene separately. For example, path 127 row 31 was the most complicated scene, in terms of land cover, containing a fair amount of each of the land cover classes and heterogeneous topography ranging from very flat regions in

the north to mountainous regions in the south. In contrast, path 128 row 30 contained no distinguishable agricultural or urban areas. Finally, path 128 row 31 contained all land cover classes as well as thick cloud cover in the southern portion of the image. The differences in each of the images allows for a better comparison of the two methods and the accuracy of their classifications.

3.3 Pixel-based Classification

For the pixel-based classification of DaMao, a supervised method was used. For display purposes, a combination of bands four, three, and two was used because of the contrast it provides between vegetated areas and non-vegetated areas, such as urban areas or barren land. Using this band combination vegetated areas are visible in various shades of red, with healthier areas showing up as brighter reds. Additionally, a NDVI image was calculated in order to better differentiate between areas of vegetation and urban or barren areas. In ENVI 4.2 the NDVI can be calculated using a tool that applies the algorithm to the entire scene. The NDVI, however, was not used to determine the actual classification.

Again, to classify the images a supervised approach was used. Training site selection was done by selecting groups of pixels that best represented areas of water, barren land, grasslands, and urban features. Training sites for urban, water, agriculture, and barren land covers were selected through visual interpretation of the image. Since there can be several variations of each of the desired land cover classes several samples were collected for each of the classes, particularly in the case of roads and rivers. Rivers have varying degrees of width and turbidity that cause the spectral signatures for the same feature to vary greatly. After selecting what was thought to be an acceptable

number of classes the image was classified. Additional training sites were added in areas that were poorly or inaccurately classified and the process was repeated.

Training sites for good, average, and poor grasslands, as well as some barren areas were collected during the summers of 2006 and 2007 by graduate students from the Rural Development Institute of the Chinese Academy of Social Sciences (RDI-CASS) in Bejing, China. Under the direction of Dr. Charles Emerson of Western Michigan University the students used handheld Global Positioning System (GPS) devices to map areas of grassland. These polygons became the training sites for the respective categories of grassland quality.

After the selection of training sites was completed the images were classified within ENVI 4.2™ using a Gaussian maximum likelihood classifier using all six visual/NIR bands. The classifier was run first without using a probability threshold and then run again using a 50% probability threshold. Without applying a probability threshold, all pixels in an image will be classified. Applying a threshold of 50% means that an unclassified pixel must have a 50% probability or greater of belonging to a class before it is classified (Richards 1999). The images classified without a threshold were used so that every pixel in the image was classified.

3.4 Object-Oriented Classification

The object-oriented classification was performed using Definiens Professional™. After importing the images into the program, the first step of the process is to select the parameters by which the segmentation will take place. Table 3.3 shows the values of each of the parameters used to segment the image and table. The selection of these parameters was a heuristic process. Each of the factors, aside from the scale factor, is on

a sliding scale of 0 to 1, meaning that the more weight you apply to the color factor, the less weight you apply to the shape factor with the same being true for the smoothness and compactness factors.

Table 3.3 Selected multiresolution segmentation input parameters

Paramter	**Value**
Color	0.1
Shape	0.9
Compactness	0.7
Smoothness	0.3
Scale Factor	10

Figures 3.4a and 3.4b show the difference in object size with a scale factor of 10 and 25 respectively. In selecting these values the focused was on individual objects that could be seen in the images, in this case water bodies such as lakes and ponds, as well as circles in agricultural areas that were clearly created by the use of center-pivot irrigation devices. These objects were focused on because there are few distinguishable objects in the homogeneous regions of grassland and desert. When looking at water bodies it is important to look for the combination that had the least amount of segmented objects that included both land and water. In agricultural areas, the focus was on how well the created objects fit the circular patterns that resulted from irrigation devices. The selection of the scale factor was also heuristic and a value of 10 were ultimately chosen because the coarse resolution of the imagery seemed to call for a low scale factor number, meaning smaller objects.

After the image was segmented, a rule base had to be created in order to classify the image. The first land cover class that was classified was urban. Because urban land cover in DaMao was so sparse urban objects were assigned to the urban class manually. Preliminary classifications of urban areas through the supervised selection of samples resulted in much confusion with the "barren" class. One reason for this is because some residential construction in is done using stucco with clay roofs, thus creating a similar signature and texture to barren regions. After manually classifying urban image objects, all water areas were then classified. Since water bodies have similar NDVI values, a rule was created that classified all image objects with an NDVI value of less than -0.2 as water. With urban and water objects set aside the remainder of the image was classified through the supervised selection of image objects. Sample objects for barren, grassland, and agriculture classes were then selected and a rule was created to classify all unclassified objects in the image using a standard nearest-neighbor classifier applied to each of the image's six layers.

Once the entire image was classified the next step was to assess the quality of the grassland objects using the NDVI values. To fully separate the grassland objects from the rest of the image objects all grassland objects were merged and then resegmented with a scale factor of 25.

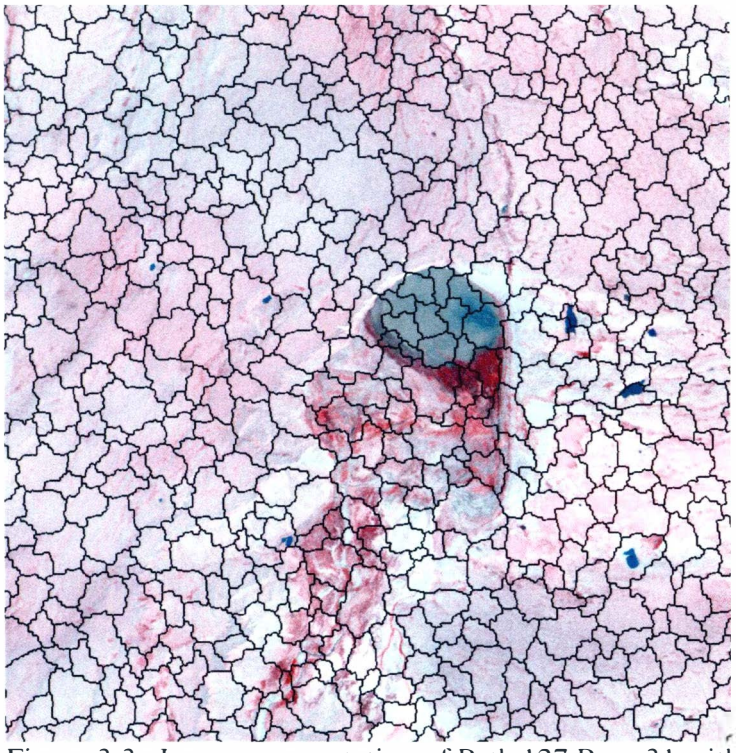

Figure 3.3a Image segmentation of Path 127 Row 31 with a scale factor of 10

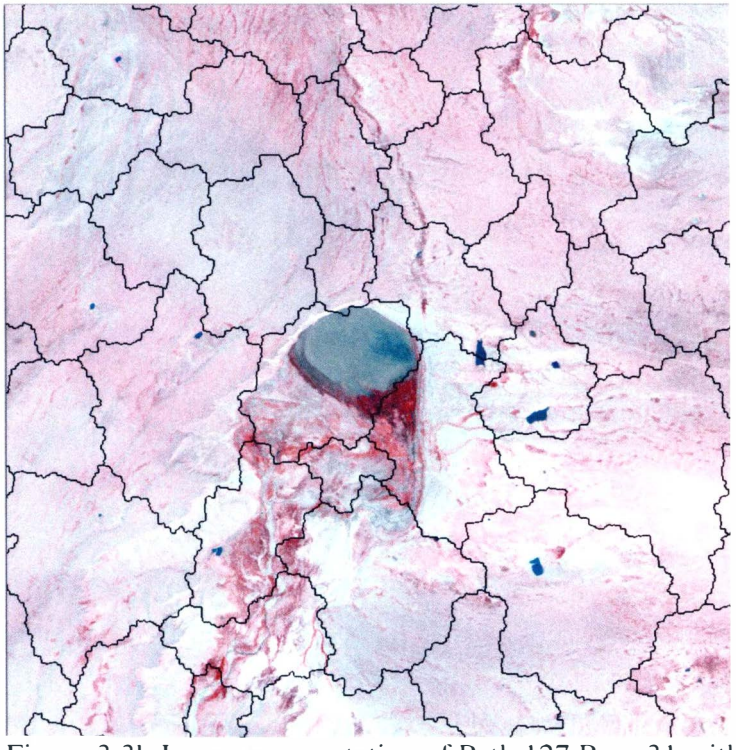

Figure 3.3b Image segmentation of Path 127 Row 31 with a scale factor of 50

A larger scale factor was used was used due to, once again, the homogeneous nature of the land cover in which there is a lack of distinguishable objects. The quality of grassland was assessed using the ranges of NDVI values that can be seen in table 3.4.

Table 3.4 Grassland quality NDVI ranges

Good Grassland	NDVI ≥ 0.30
Average Grassland	$0.11 \leq$ NDVI ≤ 0.29
Poor Grassland	NDVI ≤ 0.10

The ranges for each of the quality categories were determined from ground truth polygons collected during the summers of 2006 and 2007. Several sample sites of grassland were taken using GPS units and then classified as good, poor, or average. These polygons were then overlaid on an NDVI map of the banner which then made it possible to determine the ranges for each of the categories. In order to apply these ranges to the grassland objects, separate rules were created for the good and poor classes and all remaining unclassified objects were then classified as average.

The accuracy assessments were performed two different ways. For the pixel-based assessment, sample points were selected using a stratified random method. The sample size was based on taking a sample of 10% of the pixels proportionate to the amount of pixels in each of the sample classes. For the object-oriented assessment each of the images was segmented again using a chessboard segmentation with a scale factor of 25. A chessboard segmentation places a grid over a previous segmentation and thus does not use the color, shape, smoothness, or compactness parameters. Using this new segmentation, a new group of samples was selected for each of the land cover classes, including each of the grassland quality classes. These samples were then used to create a

Training and Test Area (TTA) mask in Definiens Professional™, which separates the samples from the image so that they can be used for the accuracy assessment. Error matrices were derived displaying the producer's accuracy, the user's accuracy, overall accuracy, and the KHAT percentage. The KHAT, or kappa statistic, is an indication of how much better the classification is than random chance.

CHAPTER 4
RESULTS AND DISCUSSION

The two techniques in this study were each applied to three Landsat 5 scenes. The data collected resulted in an output of six land use/land cover (LULC) images and six corresponding error matrices. The error matrices show the degree of misclassification among the classes. Each error matrix also contains the overall accuracy percentage and the KHAT. In some cases the Jeffries-Matusita separability measure is discussed. This is a value that measures how statistically separate samples are. The values range from zero to 2.0, with values between 1.9 and 2.0 indicating good separability and lower values indicating poor separability. This chapter will first look at the comparison of the results for each of the images separately and then discuss some of the observed positives and negatives for each of the techniques.

4.1 Path 127 Row 31

For this image the techniques produced similar accuracy results. Overall, the pixel-based methodology produced an accuracy of 64.41% and a KHAT of 0.577 (Table 4.1a) while the object-oriented image had an accuracy of 70.34% with a KHAT of 0.6255 (Table 4.2b). In table 4.1a it can be seen that there are three classes that recorded the greatest amount of misclassification using the pixel-based technique. Average grassland has a very low user's accuracy of 24.32%, which means that approximately 75% of pixels classified as average grassland were incorrectly classified, in this case, as water, agriculture, and poor grassland.

Table 4.1a Path 127 Row 31 pixel-based error matrix

	REFERENCE (Path 127, Row 31)								
MAP	Water	Agriculture	Avg Grass	Urban	Barren	Good Grass	Poor Grass	Total	User's Accuracy (%)
Water	**418**	0	0	133	0	0	0	551	75.86
Agriculture	0	**5131**	0	58	0	0	0	5189	98.88
Avg Grassland	1250	4259	**3125**	0	0	0	4216	12850	24.32
Urban	320	0	0	**2272**	194	0	0	2786	81.55
Barren	171	0	0	310	**2165**	0	0	2646	81.82
Good Grassland	0	0	0	0	0	**6758**	0	6758	100.00
Poor Grassland	0	0	0	67	0	0	**0**	67	0.00
Total	2159	9390	3125	2840	2359	6758	4216	**30847**	
Producer's Accuracy	19.36	54.64	100.00	80.00	91.78	100.00	0.00		

Sample size = 30847 **KHAT** = .577 **Overall Accuracy** = .6441

Table 4.1b Path 127 Row 31 object-oriented error matrix

	REFERENCE (Path 127, Row 31)								
MAP	Water	Agriculture	Avg Grass	Urban	Barren	Good Grass	Poor Grass	Total	User's Accuracy (%)
Water	**34**	0	0	0	0	0	0	34	100.00
Agriculture	0	**336**	4	0	5	6	1	352	95.45
Avg Grassland	0	77	**133**	2	1	1	14	228	58.33
Urban	0	2	2	**55**	32	0	13	104	52.88
Barren	1	2	0	7	**221**	0	1	232	95.26
Good Grassland	0	142	4	0	0	**36**	0	182	19.78
Poor Grassland	1	35	8	1	17	0	**84**	146	57.53
Total	36	594	151	65	276	43	113	**1278**	
Producer's Accuracy	94.44	56.57	88.08	84.62	80.07	83.72	74.34		

Sample size = 1278 **KHAT** = 0.6255 **Overall Accuracy** = 0.7034

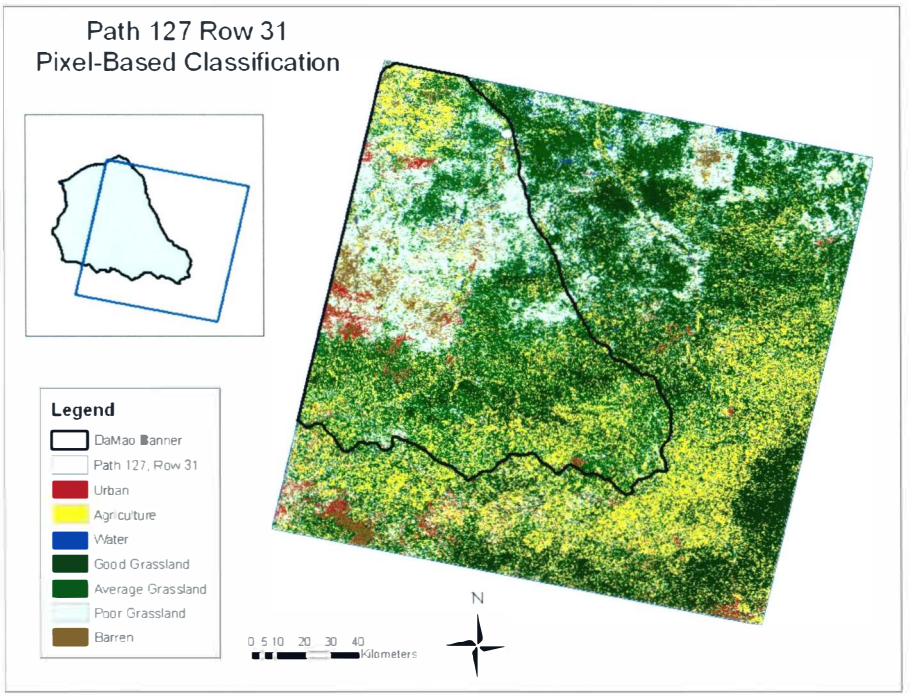

Figure 4.1a Path 127 Row 31 pixel-based LULC classification map

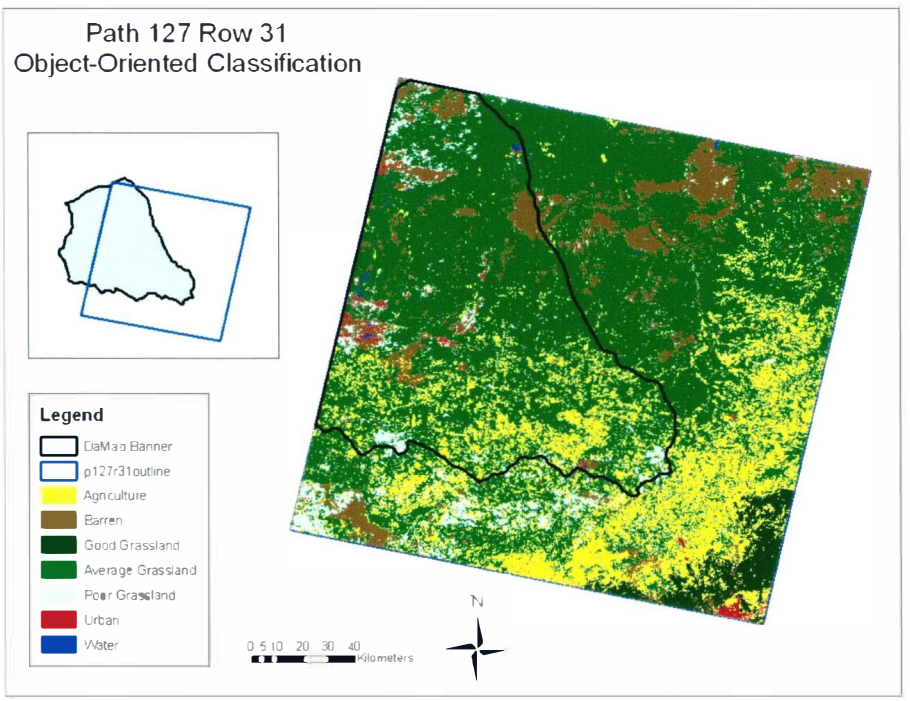

Figure 4.1b Path 127 Row 31 object-oriented LULC classification map

The Jeffries-Matusita separability value for the average grassland and agriculture classes was a very low 1.29, which shows why there was such confusion between those two classes. For average grassland and poor grassland the confusion is also apparent with a separability value of 1.44. Poor grassland also had a very low producer's and user's accuracy of zero. All of the sampled pixels that were classified as poor grassland were, in actuality, urban. Water was another class that experienced a high percentage of misclassification with a low producer's accuracy of 19.36%, which means that approximately 80% of the sampled pixels that are actually water, were classified as something else, in this case urban, barren, and especially average grassland.

Figure 4.1a shows the pixel-based LULC classification map. There are many places where the classified pixels are mixed together creating a "salt and pepper" effect. For example, throughout the areas classified as good grassland there are pixels classified as agriculture mixed in, causing some of the boundaries between grassland and agriculture to be less well defined. Another observation has to do with the confusion between urban and barren land cover. In the urban regions there are areas in which housing is made from materials such as mud and locally produced brick and clay tile. The spectral signatures created by these areas are similar to the spectral signatures of some of the barren areas. The result is concentrations of pixels classified as urban in or adjacent to barren areas. This is an issue that came up in all three sets of images.

Table 4.1b shows the error matrix for the object-oriented technique. Good grassland had a low user's accuracy of 19.78% with the most significant misclassification being with agriculture. The object-oriented methodology used in this study classified grasslands as a single class before using NDVI values with the class to determine

grassland quality. Doing this may have created some error in distinguishing between grassland objects and some agricultural objects. Another area of confusion was between poor grassland and average grassland, which could be the result of bad sample sites taken for the accuracy assessment.

Since object-oriented analysis takes the pixels in an image and segments them to create larger objects. The end result is a smoother-looking LULC map (Figure 4.1b). Additionally, there is less confusion in the map between barren and urban land use due to steps taken in the rule-based classification to separate urban areas without the use of the nearest-neighbor classifier.

4.2 Path 128 Row 30

Overall the pixel-based methodology produced an accuracy of 82.83% and a KHAT of 0.697 (table 4.2a) while object-oriented image had an accuracy of 84.93% with a KHAT of 0.8006 (table 4.2b). The high accuracy and KHAT percentages could be attributed to the fact that in this scene there is no agriculture and very little urban area which creates a less complicated land cover. In the pixel-based error-matrix the class that experienced the most confusion was urban, which has a user's accuracy of 5.29%. In this image, (figure 4.2a) land cover classified as urban was actually barren or poor grassland. The confusion with urban and poor grassland is similar to the confusion with urban and barren that was discussed earlier. Areas of very poor grassland have spectral signatures and low NDVI values that are close to that of barren. A low separability value of 1.24 between urban and poor grassland is indicative of this kind of confusion.

Table 4.2a Path 128 Row 30 pixel-based error matrix

	REFERENCE (Path 128, Row 30)							
MAP	Water	Barren	Avg Grass	Good Grass	Poor Grassland	Urban	Total	User's Accuracy (%)
Water	**436**	0	0	0	0	0	436	100.00
Barren	0	**4737**	10	0	32	0	4779	99.12
Avg. grassland	0	9	**338**	14	4	1	366	92.60
Good Grassland	0	4	11	**532**	10	0	557	95.51
Poor Grassland	0	1171	8	0	**1049**	0	2228	100.00
Urban	0	24	1	0	172	**11**	208	5.29
Total	436	5945	368	546	1267	12	**8574**	
Producer's Accuracy	99.77	79.68	91.85	97.44	82.79	91.67		
Sample size = 8574 **KHAT** = .697 **Overall Accuracy** = **.8283**								

Table 4.2b Path 128 Row 30 object-oriented error matrix

	REFERENCE (Path 128, Row 30)						
MAP	Water	Barren	Avg. grassland	Good Grassland	Poor Grassland	Total	User's Accuracy (%)
Water	1093	0	0	0	0	1093	100.00
Barren	0	1082	116	0	472	1670	64.79
Avg. grassland	0	0	570	0	0	570	100.00
Good Grassland	0	0	0	569	0	569	100.00
Poor Grassland	0	0	0	0	0	0	0.00
Total	1093	1082	686	569	472	3902	
Producer's Accuracy	100.00	100.00	83.09	100.00	0.00		
Sample size = 3902 KHAT = .8006 Overall Accuracy = .8493							

The pixel-based LULC map contains the same type of "salt and pepper" effect as path 127 row, 31 but overall does a good job of showing the detailed trend from good grassland to barren. Again the problem distinguishing between barren and urban can be seen despite the small training site sample of pixels taken to represent an almost indistinguishable populated area.

Table 4.2b shows that the object-oriented methodology had the some trouble classifying the barren land class in this image. Barren land had a user's accuracy of 64.79% with the confusion being between average grassland and especially poor grassland. The object oriented LULC map (figure 4.2b) shows much more poor grassland in areas that are classified as barren in the pixel-based LULC map. This may be because NDVI values were the primary indicator of grassland quality in the object-oriented methodology instead of ground-truth training sites in the pixel-based maps. Thus, despite the typically smoother image, the trend from good grassland to poor grassland is not as clearly depicted.

4.3 Path 128 Row 31

Overall the pixel-based methodology produced a lower accuracy of 69.08% and a KHAT of 0.6073 (table 4.3a) while the object-oriented image had an accuracy of 76.48% with a KHAT of 0.7224 (table 4.3b). In this scene a large part of the southern portion of the scene had to be masked because of cloud and their shadows. While the majority of the effects from the clouds were removed, there are some small areas along the edges that were classified as water because their black, pre-classified color was similar to the spectral signatures of water. In table 4.4a there are several notable misclassifications.

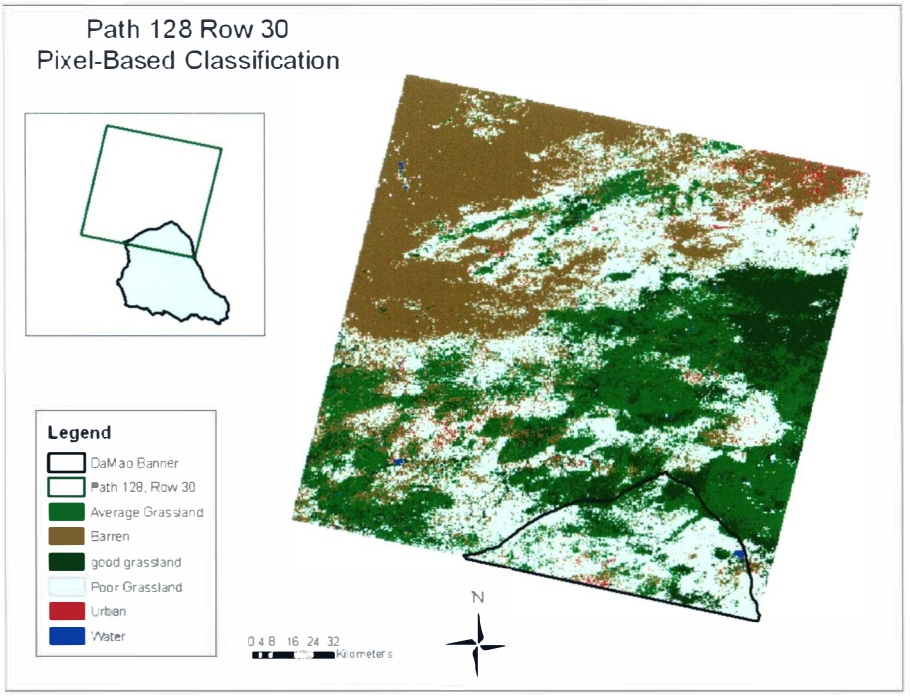

Figure 4.2a Path 128 Row 30 pixel-based LULC classification map

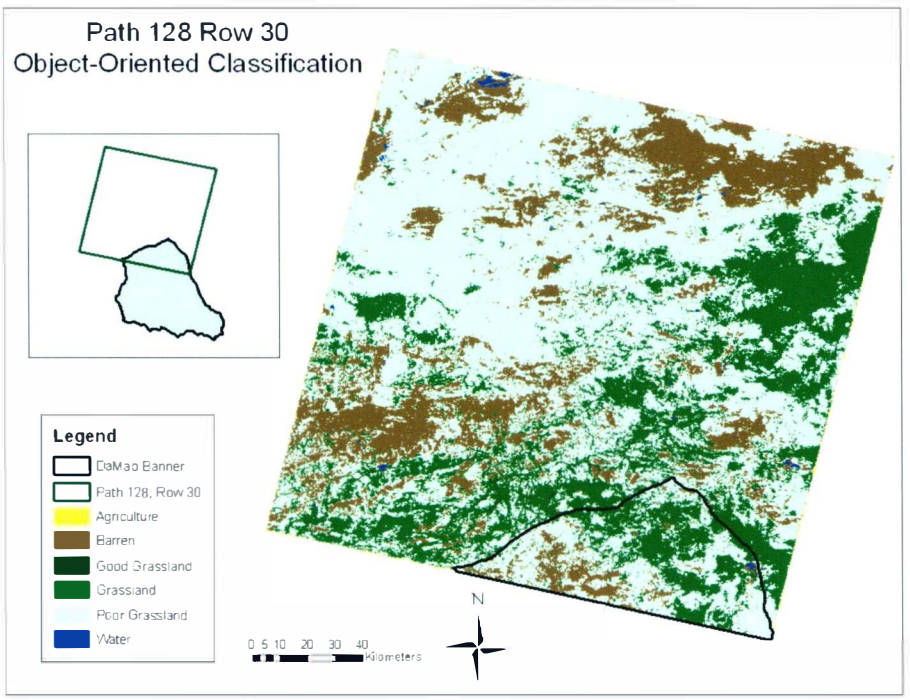

Figure 4.2b Path 128 Row 30 object-oriented LULC classification map

The barren land class has a very low user's accuracy of 18.62 with the most confusion being between average and poor grassland, and to a lesser degree, water. Additional confusion within the average and poor grassland classes and barren can be seen in the relatively low producer's accuracy percentages for each of those classes as well. Good grassland has a producer's accuracy of zero with all sampled pixels of good grassland misclassified as agricultural land. In Figure 4.3a it can be seen that there are large concentrations of urban pixels mixed in with barren land, once again pointing to the similarity of their spectral signatures and the difficulty in distinguishing between the two.

Table 4.3b shows the most notable misclassifications in the object-oriented image dealt with poor grassland, which has a producer's accuracy of 10.29%. Areas of grassland were most commonly misclassified as either average grassland or barren land which accounts for the relatively low user's accuracies of those two classes. The ability to more accurately classify the urban areas using the object-oriented methodology is evident in the LULC map (Figure 4.3b). The small urban concentrations are more easily distinguishable in the object-oriented map and there are no urban objects mixed in with barren objects. However, in no other image is barren land so closely adjacent to agricultural land which could point to an error in the sampling process.

4.4 Discussion

Object-oriented analysis performed better for land classification analysis in each of the three images, producing higher accuracy and KHAT numbers (Table 4.4). However, based on the results there are positives and negatives that can be seen for each of the techniques.

Table 4.3a Path 128 Row 31 pixel-based error matrix

	REFERENCE (Path 128, Row 31)								
MAP	Urban	Agriculture	Avg Grass	Barren	Water	Good Grass	Poor Grass	Total	User's Accuracy (%)
Urban	**1250**	0	0	0	0	0	0	1250	100.00
Agriculture	75	**1854**	167	452	0	412	0	2960	62.64
Avg Grassland	0	0	**391**	0	0	0	0	391	100.00
Barren	0	0	385	**197**	97	0	379	1058	18.62
Water	0	0	0	0	**386**	0	0	386	100.00
Good Grassland	0	0	0	0	0	**0**	0	0	0.00
Poor Grassland	0	0	0	0	0	0	**317**	317	100.00
Total	1325	1854	943	649	483	412	696	**6362**	
Producer's Accuracy	94.34	100.00	41.46	30.35	79.91	0.00	45.54		

Sample size = 6362 **KHAT** = .6073 **Overall Accuracy** = .6908

Table 4.3b Path 128 Row 31 object-oriented error matrix

	REFERENCE (Path 128, Row 31)								
MAP	Urban	Agriculture	Avg Grass	Barren	Water	Good Grass	Poor Grass	Total	User's Accuracy (%)
Urban	**68**	2	5	10	3	0	19	107	63.55
Agriculture	1	**157**	2	0	11	4	9	184	85.33
Avg Grassland	1	5	**80**	1	0	1	39	127	62.99
Barren	2	1	0	**132**	9	0	47	191	69.11
Water	0	0	0	0	**48**	0	8	56	85.71
Good Grassland	0	3	2	0	0	**109**	0	114	95.61
Poor Grassland	0	0	0	0	1	0	**14**	15	93.33
Total	72	168	89	143	72	114	136	**794**	
Producer's Accuracy	93.15	93.45	89.89	92.31	66.67	95.61	10.29		

Sample size = 794 **KHAT** = .7224 **Overall Accuracy** = .7648

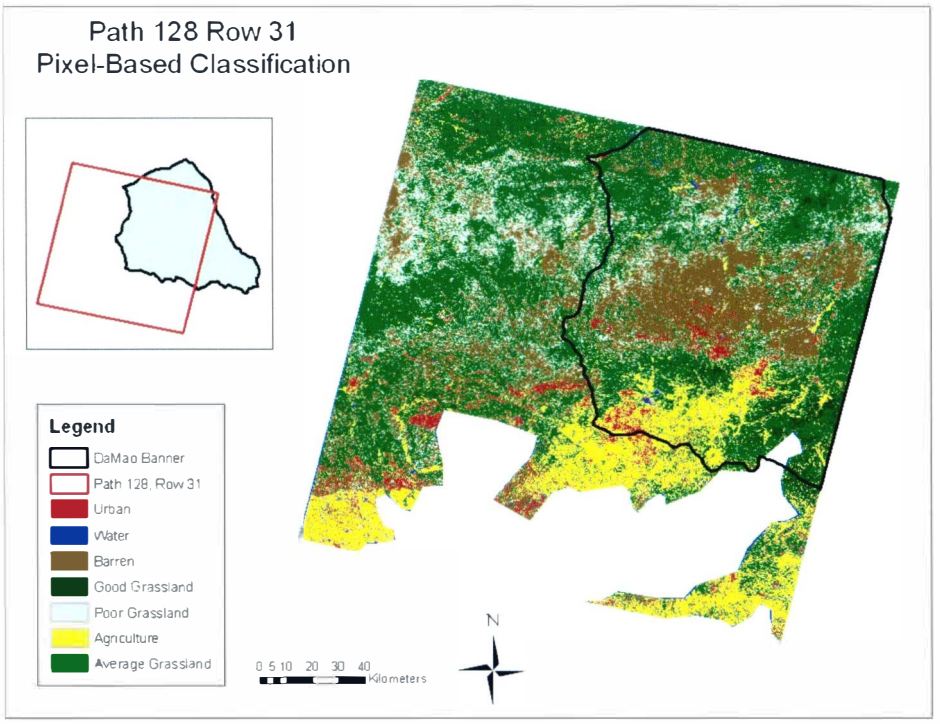

Figure 4.3a Path 128 Row 31 pixel-based LULC classification map

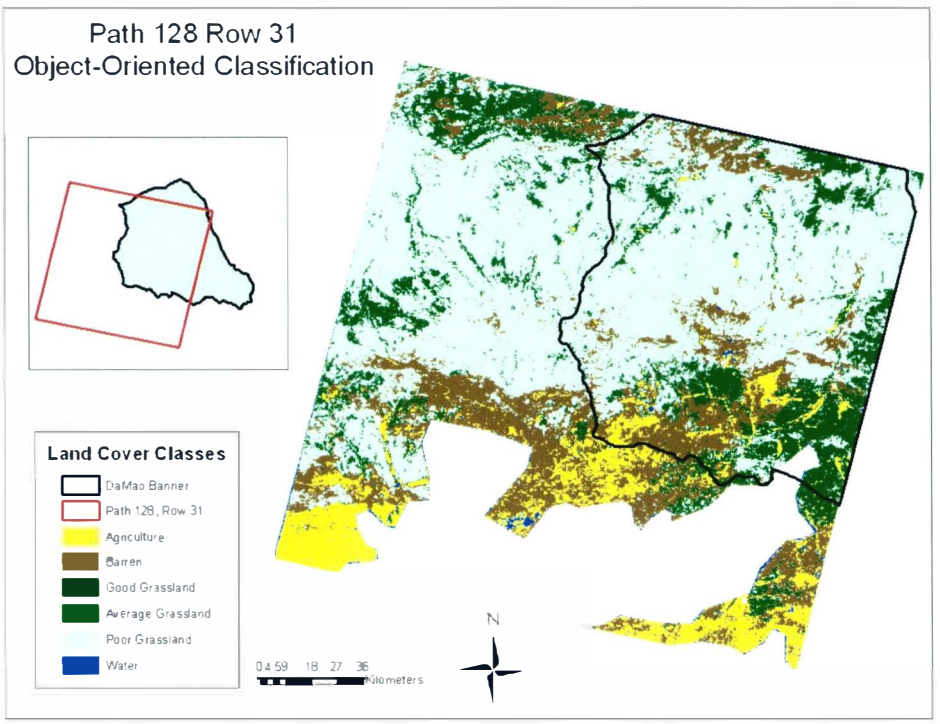

Figure 4.3b Path 128 Row 30 object-oriented LULC classification map

For the pixel-based method the positives were as follows: first, in each of the images the pixel-based method showed better detail in areas with complex land cover. This can be seen in areas where rivers are present. In such cases, rivers and stream beds may only be a pixel or two wide and many times rivers are made of mixed pixels that include water and land. In the classified maps areas where rivers are present can be seen by linear regions of higher grassland quality or agriculture. The complexity of these areas is better portrayed in the pixel-based classifications.

Table 4.4 Comparison of KHAT values

Image	Object-oriented	Pixel-based
Path 127 Row 31	0.6255	0.5770
Path 128 Row 30	0.8006	0.6970
Path 128 Row 31	0.7224	0.6073

A second positive is that the pixel-based analysis appears to do a better job at presenting the pixel-to-pixel variability of grassland quality across the entire Landsat scene. It presents a better idea of the trend from good grassland to poor grasslands and eventually to barren areas.

There are a few negatives to pixel-based analysis. Since pixel-based analysis relies on spectral signatures to classify pixels, there is no consideration of contextual or spatial factors when classifying. Additionally, there was a significant "salt and pepper" effect in the LULC maps that results in unclear images. This can be cleaned up using a "majority filter" which smoothes the image and removes some of the pixel-to-pixel variance.

The positives for the object-oriented analysis were: first, a much smoother, easy to read map as a result of classifying larger image objects instead of individual pixels. Second, the hierarchical approach allowed for grassland quality classes to be classified separately from the rest of the classification process, thus allowing for less confusion with other classes. The ability to individually classify purely urban objects was a plus as it removed some of the confusion between barren and urban areas. On the negative side, there was numerous times in which segmenting an image using Definiens Professional™ or Definiens Professional™ for Large Data Handling (LDH) caused the program and the computer to crash. Solutions to this would be using an outline of the study area to mask the satellite images. Eventually, however, all segmentations were performed.

CHAPTER 5
SUMMARY AND CONCLUSIONS

5.1 Summary

This study conducted a comparative analysis of the performance of object-oriented and pixel-based image analysis to classify land use/land cover and assess grassland quality in DaMao Banner, China, using Landsat 5 satellite imagery. The results of the study found that the object-oriented methodology yielded higher overall accuracy and KHAT percentages in each of the three images. While there are several ways to improve accuracy results, such as increasing the number of training sites or utilizing different vegetation indices, the results found were consistent with those of similar studies. Object-oriented analysis also allows for the use of texture, shape, and contextual features to increase accuracy results. It is important to note however that this is just one specific case in which object-oriented methods outperform pixel-based methods and that the results are to be interpreted as such.

5.2 Future Research

The merits of each of these techniques should continue to be compared on different type of land cover and different types of imagery. Comparisons on how the two techniques perform when classifying forest/nonforested area or urban landscapes and classifying land use/land cover in different climatic zones are just two examples of what needs to be seen if one technique can ever be definitely declared as "better". However, with the problems and issues related to analysis of land use/land cover and land degradation, the applications for this type of comparative study are endless.

BIBLIOGRAPHY

Baatz, M. and ten others, 2004, eCognition Professional 4.0 User Guide. Munchen,Germany: Definiens Imaging, 60-76.

Benz, U.C., Hofmann, P., Willhauck, G., Lingenfelder, I., and Heyen, M., 2004, Multi-resolution, object-oriented fuzzy analysis of remote sensing data for GIS-ready information. *ISPRS Journal of Photogrammetry and Remote Sensing*, **58**, 239-258.

Brogaard, S., Runnstrom, M., and Seaquist, J.W., 2005, Primary production of Inner Mongolia, China, between 1982 and 1999 estimated by a satellite data-driven light use efficiency model. *Global and Planetary ChangeI, 45, 313-332.*

Campbell, J.B., 2002, Introduction to Remote Sensing. New York, NY; The Guilford Press, 323-339.

Chander, G., and Markham, B., 2003, Revised Landsat-5 TM radiometric Calibration procedures and postcalibration dynamic ranges. *IEEE*

Di Bella, C., Faivre, R., Ruget, F., and Seguin, B., 2005, Using VEGETATION satellite data and the crop model STICS-Prairie to estimate pasture production at the national level in France. *Physics and Chemistry of the Earth*, **30**, 3-9.

Erasmi, S., Twele, A., Ardiansyah, M., Malik, A., and Kappas, M., 2004, Mapping deforestation and land cover conversion at the rainforest margin in central Sulawesi. *EARSeL eProceedings.*

Inner Mongolia Autonomous Region Bureau of Statistics, 2007, Inner Mongolia Statistical Yearbook. Beijing, China; China Statistics Press, 612-613.

Inner Mongolia Project Management Office, 1998, Implementation Plan for Land Acquisition and Compensation. *World Bank China Western Reduction Project*, **3**, 1-24.

Jensen, J.R., 2005, Introductory Digital Image Processing. Upper Saddle River, NJ;Prentice-Hall, 337-401.

Kressler, F.P., Steinnocher, K., and Franzen, M., 2005, Object-oriented Classification of orthophotos to support update of spatial databases. *IEEE Explore*, **5**, 253-256.

Laliberte, A.S., Rango, A., Havstad, K.M., Paris, J.F., Beck, R.F., McNeely, R., and Gonzalez, A.L., 2004, Object-oriented image analysis for mapping shrub encroachment from 1937 to 2003 in southern New Mexico. *Remote Sensing of the environment*, **93**, 198-210.

Milton, S.J., Dean, W.R.J., du Plessis, M.A., and Siegfried, W.R., 1994, A conceptual model of arid rangeland degradation. *BioScience*, **44**, 70-76

Navulur, K., 2007, Multispectral Image Analysis Using the Object-Oriented Paradigm. New York, NY; CRC Press.

Paruelo, J.M., and Lauenroth, W.K., 1995, Regional patterns of normalized difference vegetation index in North American shrublands and grasslands. *Ecology*, **76**, 1888-1898.

Platt, R.V. and Goetz, A.F.H., 2004, A comparison of AVIRIS and synthetic Landsat data for land use classification at the urban fringe. *Photogrammetric Engineering and Remote Sensing*, **70**, 813-819.

Platt, R.V., and Rapoza, L., 2008, An Evaluation of an Object-Oriented Paradigm for Land Use/ Land Cover Classification. *The Professional Geographer*, **60**, 87-100.

Richards, J.A., 1999, Remote Sensing Digital Image Analysis. Berlin, Germany; Springer-Verlag, 240.

Santos, T., Tenedoria, J.A., Encarnacao, S., Rocha, J., 2006, Comparing pixel vs. object based classifiers for land cover mapping with Envisat-MERIS data. Warsaw, Poland; *EARSeL Symposium*, March 26.

Schowengerdt, R.A., 1997, Remote Sensing: Models and Methods for Image Processing.San Diego, CA; Academic Press, 183-184, 403-426.

Shanmugam, S., Lucas, N., Phipps, P., Richards, A., and Barnsley, M., 2003, Assessment of Remote Sensing Techniques for Habitat Mapping in Coastal Dune Ecosystems. *Journal of Coastal Research*, **19**, 64-75.

Townshend, J.R.G., Huang, C., Kalluri, S.N.V., Defries, R.S., and Liang, S., 2000, Beware of per pixel characterization of land cover. *International Journal of Remote Sensing,* **21**, 839-843.

Veeck, G., Emerson, C., Li, Z., Yu, F., and Haipeng, Z., 2007, Global trade and

local herders: An environmental economic analysis of husbandry in DaMao Banner, Inner Mongolia, People's Republic of China. *Facing East facing West Conference 2007.*

White, R., Murray, S., and Rohweder, M., 2000, Pilot analysis of ecosystems: Grassland ecosystems. *World Resources Institute*. Accessed: 05/20/2008. http://www.wri.org/publication/pilot-analysis-global-ecosystems-grassland-ecosystems#publication_tabs-2

Yijun, C., and Hussin, Y.A., 2003, Object-Oriented Classifier for Detection of Tropical Deforestation Using LandSat ETM+ in Beray, East Kalimant, Indonesia. *Map Asia Conference 2003 – Natural Resource Management.*

Zha, Y., Gao, J., Ni, S., Liu, Y., Jiang, J., and Wei, Y., 2003, A spectral reflectance based approach to quantification of grassland cover from Landsat TM imagery. *Remote Sensing of the Environment*, **87**, 371-375.